iScience

CellPress
OPEN ACCESS

Article

Adsorption and desorption behavior of Zn^{2+} in a flow-through electrosorption reactor

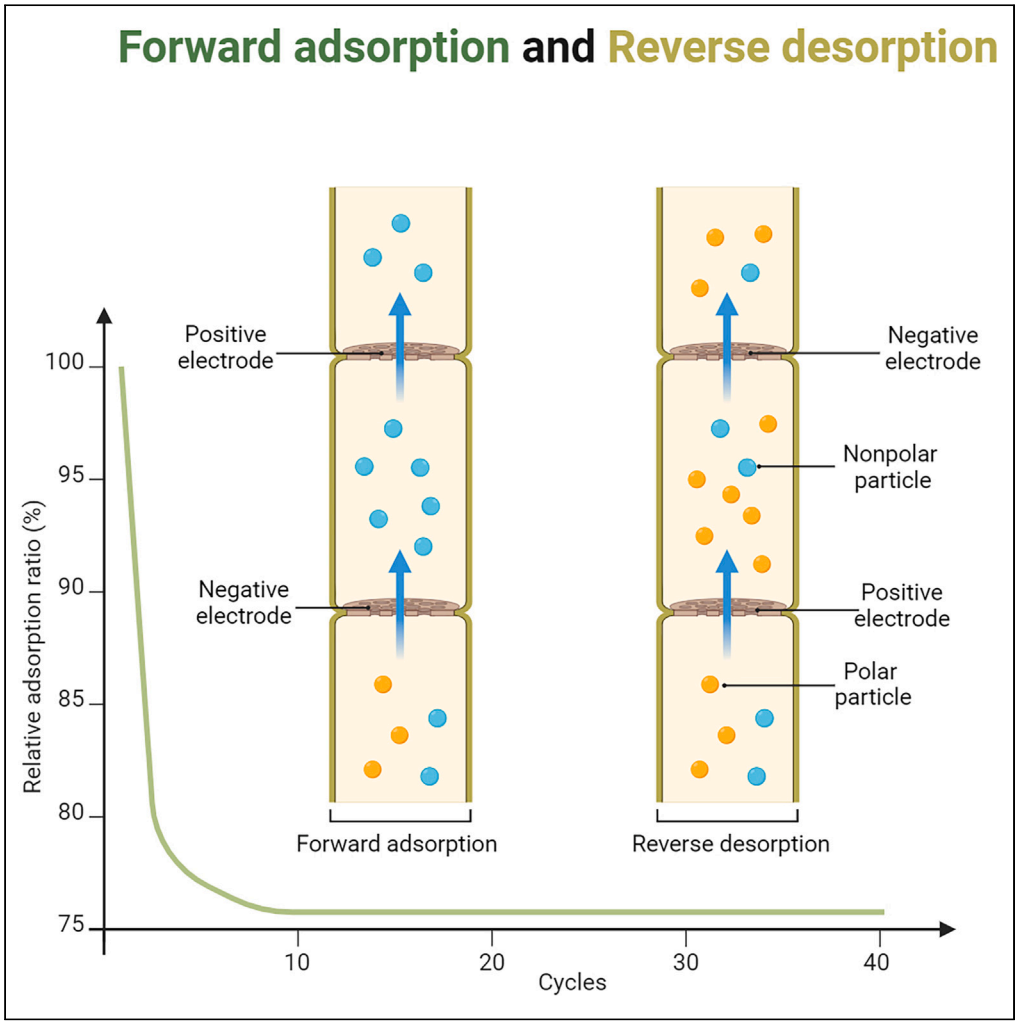

Yusen Dong, Manci Jiang, Jing Zhao, Fei Zhang, Shaohua Ma, Yang Zhang

18810887900@163.com

Highlights

A flow-through electrosorption reactor is proposed

Found the most suitable conditions for this module

Various models were used to describe the adsorption process

Adsorption efficacy is highly reproducible over multiple cycles

Dong et al., iScience 27, 109514
April 19, 2024
https://doi.org/10.1016/j.isci.2024.109514

iScience

CellPress
OPEN ACCESS

Article

Adsorption and desorption behavior of Zn^{2+} in a flow-through electrosorption reactor

Yusen Dong,[1,2,*] Manci Jiang,[1] Jing Zhao,[1] Fei Zhang,[1] Shaohua Ma,[1] and Yang Zhang[1]

SUMMARY

As heavy metal industrial wastewater increases in volume and complexity, we need more efficient, cheaper, and renewable technologies to curb its environmental impact. Compared to advection electrosorption, through-flow electrosorption is a hotspot technique that makes more efficient use of the adsorption capacity of activated carbon fiber mats. A cascade flow-through electrosorption assembly based on activated carbon fiber was used to obtain the best adsorption of Zn^{2+} in water at a voltage of 2 V, pH value of 8, plate spacing of 3 mm, and temperature of 15°C. The process is more closely fitted to the secondary adsorption kinetic equation and the Langmuir equation. The adsorption capacity of the module decreases at a progressively slower rate with the number of cycles and will eventually retain 75% of its peak value with significant regenerability. The study of this module can provide technical support for treating heavy metal wastewater.

INTRODUCTION

With the continuous development of the economy, the discharge of various types of heavy metal wastewater that harms the environment cannot be ignored.[1,2] Significant differences exist in the content of Zn^{2+} in wastewater produced by different industries, ranging from 50 mg/L in the electroplating industry to 20,000 mg/L in the pharmaceutical industry where zinc acetate is widely used. To cope with the environmental pressure caused by the expanding heavy metal wastewater, researchers have proposed technologies such as chemical precipitation, ion exchange, membrane separation, distillation, adsorption, and others.[3] Adsorption technology has been widely used in the field of water treatment for its simple process control. The essence of adsorption water purification technology is the non-homogeneous migration process of pollutants between the adsorbent and the wastewater.[4–6] However, traditional adsorption technology often suffers from secondary pollution, low recovery rate, and short life span in practical applications. In contrast, the emergence of electroabsorption technology, also known as capacitive deionization technology in recent years, is considered a highly promising water treatment strategy due to its high efficiency, low energy consumption, and simple regeneration process of the adsorbent.[7–9]

Heavy metal wastewater containing zinc, chromium, lead, and copper generated by human industrial activities can have bioaccumulative effects and persistent ecological problems.[10] Zinc metal is commonly used in the production of industrial products such as alkaline carbonic acid plating for corrosion protection, alloy preparation, plastics, batteries, lubricants, and flame retardants.[11] The concentration of zinc in aquatic plants and animals can reach more than a thousand times the background value, showing an extremely strong bioaccumulation effect. Excessive intake of zinc can cause zinc toxicity in the body leading to symptoms of stomach ulcers, stomach bleeding, and disorders of cholesterol metabolism.[12,13]

Flexible activated carbon fibers have attracted extensive research in the field of electroabsorption because of their excellent electrical and thermal conductivity, high-temperature resistance, low thermal expansion, and stable chemical properties.[14] It has been shown that material modification operations for activated carbon fibers can effectively enhance core parameters such as system electroabsorption efficiency, specific surface area, porosity, pore size distribution, and selectivity. The l-cysteine-modified activated carbon fiber could reach a maximum adsorption capacity of 179.53 mg/g for lead ions as deduced by the Langmuir model.[15] Electrochemical analysis of camphor carbon fume by cyclic voltammetry with constant current charge-discharge showed that the doping of nitrogen significantly increased its specific capacitance and caused it to exhibit multilayer adsorption on non-homogeneous surfaces following Freundlich.[16] As another efficient adsorption material, multiwall carbon nanotubes can improve the stability of emulsion liquid membrane (ELM) by approximately 20% when effectively applied, reduce the swelling ratio of emulsion by 42%, and increase the mass transfer coefficient by 4.746% when cooperating with surfactants.[17,18] On the other hand, this saturated adsorption device enriched with many charges is often regarded as an energy storage device. Some researchers have attempted to expand it into the field of nanogenerators and non-destructively monitor its parameters such as voltage, current, temperature, etc., which broadens the relevance for its extended applications.[19–21] A large number of studies have focused extensively on the electrosorption properties of carbon-based adsorbent materials and their behavior under typical modifications but have not focused on the interaction of flowing water with carbon materials.

[1]Beijing Institute of Aerospace Testing Technology, Beijing 100074, China
[2]Lead contact
*Correspondence: 18810887900@163.com
https://doi.org/10.1016/j.isci.2024.109514

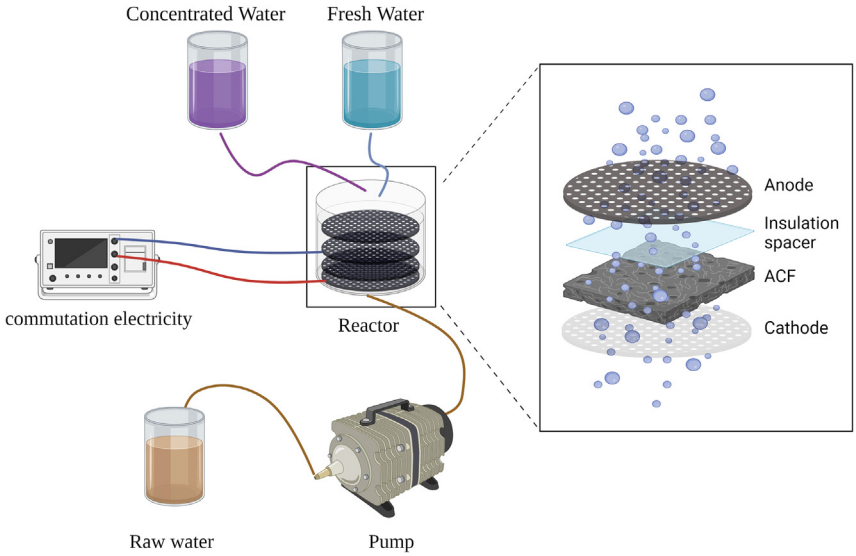

Figure 1. Zn^{2+} adsorption test equipment

Motivated by the aforementioned promising research, this paper constructs a flow-through (the direction of water flow completely penetrates the adsorbent material) electrosorption reactor different from the common flow-by (the direction of water flow is exactly parallel to the adsorption material) reactor. The flow-through electrosorption reactor was tested to have a better response to Zn^{2+} electrosorption efficiency by reasonable process control when filled with activated carbon fiber electrodes. Therefore, this paper hopes to provide intentional technical support for the innovative progress of electroabsorption technology.

RESULTS

The reactor used in the experiment is shown in Figure 1. The Zn^{2+} adsorption behavior of the flow-through reactor-activated carbon fiber mat system was investigated experimentally at different pole plate spacing, voltage, pH, temperature, and feedwater concentration.

Effect of polar plate spacing on the behavior of electrosorption of Zn^{2+}

Figure 2 depicts the effect of pole plate spacing variation on Zn^{2+} (400 mg/L) in the electrosorption wastewater. As Table 1 shows, in the direction of the timescale, the change in the electrosorption Zn^{2+} process was less significant after 60 min ($p = 0.033 > 0.01$) and lost significance after 70 min ($p = 0.053 > 0.05$) (p is used to describe the significance of the indicator for evaluating the correlation of data between groups, the same in the following text.). Taking the 60 min at which the time of the adsorption process begins to decrease toward the difference as the

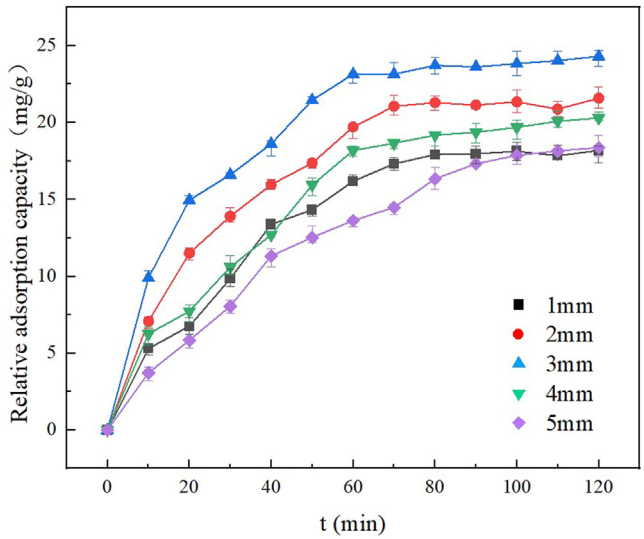

Figure 2. Influence of polar plate spacing on the effect of electro-absorption

Table 1. Results of experimental data analysis of Zn electrosorption at different plate spacings

parameters	1 mm	2 mm	3 mm	4 mm	5 mm
The ratio of 20 min adsorption amounts to the maximum value	41.98%	58.38%	64.94%	34.26%	47.65%
Significance of differences in data between groups, comparison with 3 mm experimental group	0.002[b]	0.013[a]	–	0.021[a]	0.018[a]

[a]means that the difference between the comparative data is significant.
[b]means that the difference between the comparative data is extremely significant, the same in the following table.

assumed endpoint of adsorption, most of the adsorption process is completed within 20 min of the beginning of adsorption, and this trend increases as the pole-plate spacing approaches 3 mm.[8,17,22] The adsorption behavior starts with more adsorption sites on the surface of the activated carbon fiber mat, and the adsorption moves faster toward the equilibrium, as the adsorption process goes on, the number of sites on the surface of the activated carbon fiber mat gradually decreases and finally approaches the equilibrium, and the adsorption capacity no longer changes significantly. The comparison between the different electrode spacing groups demonstrated that the 3 mm electrode spacing had a significant advantage in relative adsorption of 23.14 mg/g and differed significantly from the other spacing configurations. The relative adsorption amounts between groups at the same time during the process of electrosorption showed a positively skewed distribution, reaching a large value of significance near the equilibrium point of adsorption ($p = 0.997$). This result reveals that the electrode plate spacing, i.e., the thickness of the porous insulating mat, should be guaranteed to be 3 mm, for the flow-through electrosorption of Zn^{2+}.

In the chronological direction, the electroabsorption gradually moves toward equilibrium, and the activated carbon fiber mat gradually reaches the adsorption equilibrium under the electric drive, which shows a gradual decrease in the rate of change of the relative adsorption amount. On the other hand, there was a significant increase in relative adsorption with decreasing pole plate spacing but caused a significant decrease in relative adsorption at spacing below 3 mm. This may be because decreasing the electrode spacing in a certain range of flow-through stacked electrodes can enhance the electric field strength, reduce the mass transfer resistance, enhance the mass transfer efficiency, and bring about a certain increase in the adsorption capacity. However, the continued reduction of the electrode spacing may cause short-circuiting of some electrodes and the loss of electrically driven adsorption capacity;[23] at the same time, the lower electrode spacing also makes the "cavity" effect of the porous electrode plate increase, and the local electric field strength is lower, even resulting in the interaction effect between the multi-layer electrode stack, which causes the further reduction of the relative adsorption capacity.[24,25]

Influence of polar plate voltage on the effect of electro-absorption

Figure 3 depicts the response state of the voltage variation for Zn^{2+} (400 mg/L) in the electrosorption wastewater. As Table 2 shows, in the direction of the timescale, the process of electrosorption lost significance at 40 min ($p = 0.359 > 0.05$) and then recovered until it lost significance again at 90 min ($p = 0.782 > 0.05$). The endpoint of adsorption was 90 min with a significant decrease in the start of the adsorption process, and most of the adsorption process was completed within 40 min, and the trend increased gradually with the increase of voltage to 2.5V. Comparison between groups with different electrode voltages showed that the operating voltage of 2 V had the relative adsorption

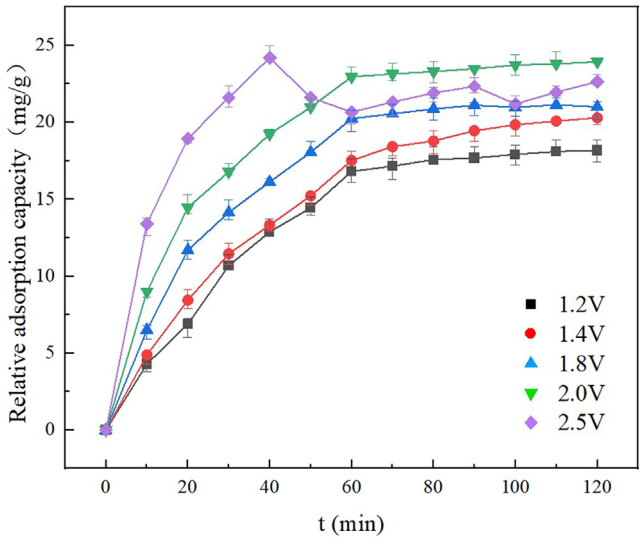

Figure 3. Influence of the pole-plate voltage on the electro-absorption effect

Table 2. Results of experimental data analysis of Zn electrosorption at different pole-plate voltage

parameters	1.2 V	1.4 V	1.8 V	2.0 V	2.5 V
The ratio of 40 min adsorption amounts to the maximum value	60.46%	58.90%	67.01%	71.47%	96.71%
Significance of differences in data between groups, comparison with 2 V experimental group	0.005**	0.027*	0.017*	–	0.04*

performance of 23.93 mg/g dominant and was significantly different from the other experimental groups. Unlike other experimental studies, the peak relative adsorption capacity of 24.2 mg/g was reached at 40 min at an operating voltage of 2.5 V and then decreased. At the loss of significance of the adsorption process (not counting the specific 2.5 V experimental group), the data were positively skewed between the electroabsorption groups ($p = 0.831$). This result suggests that for Zn^{2+} flow-through electrosorption, the operating voltage should be as close to 2 V as possible and ensure that it does not exceed 2.5 V.

The ability of flow-through electrosorption of Zn^{2+} gradually increases as the operating voltage increases continuously toward 2 V. However, the relative adsorption amount rises rapidly when the voltage reaches 2.5 V and then decreases rapidly, during which a large number of fine bubbles are generated in the bilateral pole plates. It indicates that the mass transfer capacity of the electrosorption process gradually increases with the increase of voltage, bringing about the increase of adsorption amount, but the continued increase of voltage will bring about the side reaction of electrolytic water to produce a large number of micro-foam bubbles, which will encroach on a large number of adsorption sites and destroy the double electric layer structure, resulting in the da of relative adsorption amount.[8,26]

Effect of pH on the electroabsorption

Figure 4 and Table 3 depict the results of the pH change response of Zn^{2+} by flow-through electroabsorption. The relative adsorption amount increased and then decreased with increasing pH and reached a maximum value of 24.79 mg/g at pH = 8. The relative adsorption amount obeyed a positively skewed distribution along the increasing pH direction ($p = 0.347$) with significant intergroup variability. Flow-through electroabsorption of Zn^{2+} should maintain its applied pH between 6 and 8.

Flow-through electrosorption at low pH will behave as H^+ competing with metal ions for adsorption, consuming a large number of activated carbon fiber mat surface sites, while consuming a large number of charges leading to changes in the composition of the double electric layer. In the process of gradually increasing pH, most metal ions will behave as precipitates formed with OH^-, the colloidal state within the solution system, and most of them are negatively charged, leading to the migration of metal colloids to the positive pole within the system, which reduces the relative adsorption of metal ions by activated carbon fiber mats.[27–30]

Effect of temperature on electrical absorption

Figure 5 depicts the results of the flow-through electrosorption response to temperature changes. As Table 4 shows, in the temporal direction, the adsorption process lost significance after 60 min ($p = 0.058 > 0.05$), taking it as the endpoint, most of the adsorption processes were

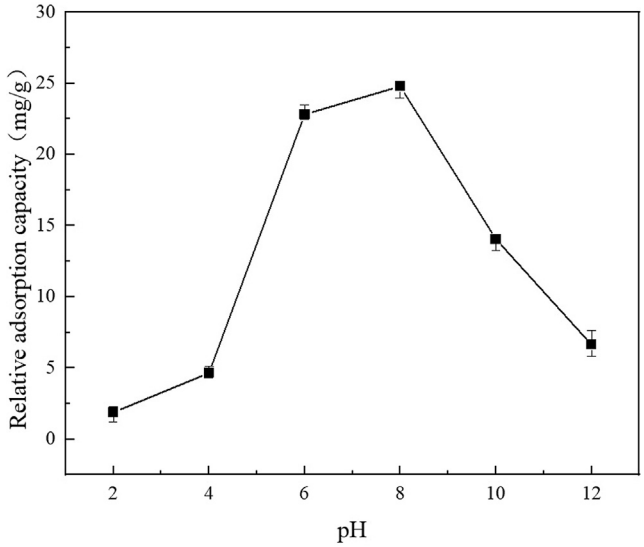

Figure 4. Effect of pH on the electroabsorption

Table 3. Results of experimental data analysis of Zn electrosorption at different pH

Parameters(pH)	2	4	6	8	10	12
Significance of differences in data between groups, comparison with 8(pH) experimental group	0.041*	0.017*	0.035*	–	0.0072**	0.0035**

completed within 40 min and there was a tendency for this phenomenon to decrease with increasing temperature. Comparison between different operating temperature groups showed that the ambient temperature of 15°C could reach relative adsorption of 23.33 mg/g and was significantly different from other temperatures. During the process of electrosorption, the relative adsorption between the groups at the same time (0–40 min) showed a negatively skewed distribution, reaching a large positive significant value near the adsorption equilibrium point ($p = 0.938$). This result shows that flow-through electrosorption should ensure a temperature of 15°C.

To a certain extent, raising the solution temperature will enhance the momentum of the particles in it, at which point the resistance of the applied electric field to drive their migration will be raised. Flow-through electrosorption exhibits a decrease in relative adsorption capacity at higher temperatures, which may be due to the difficulty of adsorption due to the increased irregular motion of Zn^{2+} at higher temperatures and the possible exothermic adsorption reaction of Zn^{2+} by electrosorption.[31,32]

Effect of substrate concentration on electrical absorption

Figure 6 depicts the results of the performance of flow-through electrosorption under different substrate concentration conditions. As Table 5 shows, in the direction of the timescale, the process of electrosorption of metal ions lost its significance of change after 60 min ($p = 0.352 > 0.05$), taking it as the endpoint of adsorption, most of the adsorption process was completed within 30 min, and this trend decreased as the substrate concentration moved away from 100 mg/L. Comparison between different substrate concentrations showed that 400 mg/L had a significant advantage in relative adsorption of 22.96 mg/g and was significantly different from other concentration configurations. During the adsorption process, the relative adsorption amounts between groups at the same time were positively skewed and reached a high normal significance at the adsorption equilibrium point ($p = 0.779$). This result shows that for the flow-through electrosorption of metal ions, the feedwater concentration of the substrate can be appropriately increased within a certain range.

A certain amount of adsorbent continuously improves its adsorption capacity and mass transfer capacity with the increase in the concentration of adsorbate. At the same time, the metal ions in the liquid phase will have a higher chance to contact the adsorbent and be captured under the action of the adsorption force enhanced by the electric field force. However, exorbitant substrate concentration will increase produced water concentration at a certain amount of adsorbent, so the coordination relationship between substrate dosing concentration and the adsorbent amount should be properly considered in engineering applications.[32–35]

Adsorption kinetics

As an internal factor influencing flow-through electrosorption, the variation of electrode spacing is more economical than changing the voltage and can also provide more valuable technical support for the engineering application of the technology. In this section, the

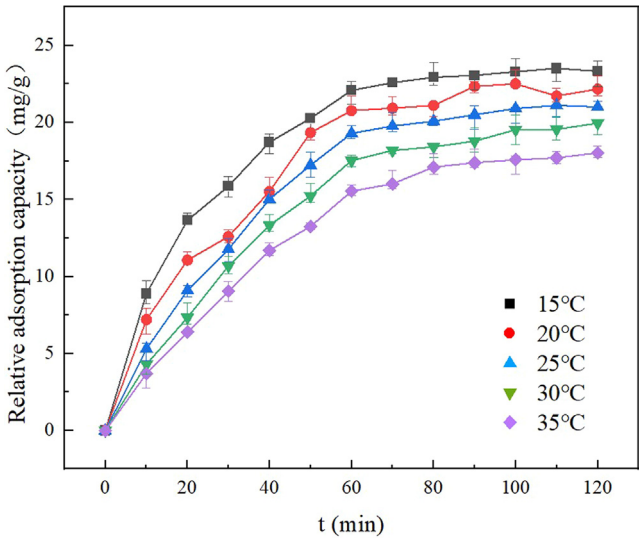

Figure 5. Effect of temperature on electrical absorption

Table 4. Results of experimental data analysis of Zn^{2+} electrosorption at different temperature

parameters	15°C	20°C	25°C	30°C	35°C
The ratio of 40 min adsorption amounts to maximum value	84.70%	74.72%	77.86%	76.08%	75.23%
Significance of differences in data between groups, comparison with 15°C experimental group	–	0.014*	0.001*	0.002**	0.001**

quasi-primary kinetic model, quasi-secondary kinetic model, and intraparticle diffusion model are fitted for different pole-plate spacing conditions. The kinetic equation is as follows.

$$\ln(q_e - q_t) = \ln q_e - k_1 t \quad \text{(Equation 1)}$$

$$\frac{t}{q_t} = \frac{1}{k_2 q_e^2} + \frac{t}{q_e} \quad \text{(Equation 2)}$$

$$q_t = k_p t^{0.5} + C \quad \text{(Equation 3)}$$

In the formula, q_e is the adsorption capacity at equilibrium and q_t is the adsorption capacity at time t, mg/g; k_1(min-1) is the quasi-level kinetic constant, k_2(g/(mg·min)) is the quasi-secondary kinetic constant; c is a constant.

Figure 7A shows the results of the quasi-level dynamic fit and Figure 7B shows the results of the quasi-level two dynamic fit. The fitted parameters are shown in the following table.

The quasi-secondary kinetic (Figure 7B) fit of the adsorption behavior of activated carbon fibers on Zn^{2+} has a higher R^2 value then Quasi first-order kinetic (Figure 7A) and k decreases with the increase of the pole plate spacing.[36] The time required for adsorption to reach equilibrium gradually increased with increasing pole plate spacing, and the adsorption behavior was a complex chemisorption process with a shared electron pair or electron exchange process between the activated carbon fiber mat and Zn^{2+}. The quasi-secondary adsorption kinetic model provides more explanation of the adsorption behavior and can better describe the electrosorption behavior of Zn^{2+} on activated carbon fiber mats.[37,38]

The results of fitting the intraparticle diffusion model with different pole-plate spacing are shown in Figure 8.

The fitted curve does not pass through the origin and is bipartite, with the first segment having a higher slope. It can be seen that flow-through electrosorption is an adsorption process controlled by both internal diffusion and membrane diffusion. In the first 30 min, the system is mainly in the surface diffusion phase, and the adsorption rate is controlled by the internal diffusion step, with a high adsorption rate and strong mass transfer dynamics, and a larger k value represents a faster adsorption rate.[39] In the second 30 min, the surface spots of the activated carbon fiber mat were gradually saturated, the concentration of metal ions in the liquid phase was gradually reduced, the adsorption

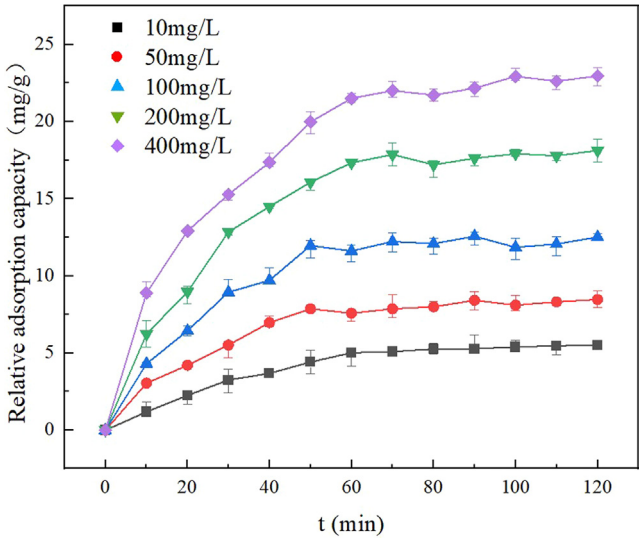

Figure 6. Effect of substrate concentration on electrical absorption

Table 5. Results of experimental data analysis of Zn electrosorption at different substrate concentrations

parameters	10 mg/L	50 mg/L	100 mg/L	200 mg/L	400 mg/L
The ratio of 30 min adsorption amounts to maximum value	64.87%	72.92%	77.09%	74.11%	71.04%
Significance of differences in data between groups, comparison with 400 mg/L experimental group	0.000**	0.000**	0.000**	0.001**	–

rate was controlled by the membrane diffusion step together with the internal diffusion step, and the adsorption gradually moved toward the steady-state process.[40]

Adsorption thermodynamics

The Langmuir and Freundlich models are used to describe monolayer homogeneous and non-homogeneous adsorption systems, respectively. The fitting results are shown in Figure 5 and Table 3.

$$\frac{C_e}{q_e} = \frac{C_e}{q_m} + \frac{1}{bq_m} \quad \text{(Equation 4)}$$

$$ln\, q_e = ln\, K_f + \frac{1}{n} ln\, C_e \quad \text{(Equation 5)}$$

In the formula, q_e is the adsorption capacity at equilibrium, mg/g; q_m is the maximum adsorption capacity, mg/g; b is the adsorption equilibrium constant and L/mg; n and k are empirical constants.

The R^2 values of the fitted Langmuir model were 0.97782, 0.97671, and 0.98546 at 15°C, 25°C, and 35°C conditions, respectively, compared to 0.94941, 0.92786, and 0.9382 of the Freundlich model, according to which it was judged that the adsorption of Zn^{2+} by flow-through electrosorption was more consistent with the Langmuir model, and the system within predominantly chemisorption-dominated monolayer adsorption.[41–44] The q_m values were 14.04009, 10.60852, and 9.42945 at the adsorption temperatures of 15°C, 25°C, and 35°C, respectively, and the adsorption amount decreased gradually with the increase in temperature, indicating that the reaction of Zn^{2+} electroabsorption is exothermic and the appropriate temperature reduction helps the reaction to proceed positively. On the contrary, desorption would be a heat-absorbing reaction, and the application of this technology in practice should be carefully dependent on the amount of ambient temperature.

Zn^{2+} substrate concentration of 100 mg/L for Figure 6. The adsorption process's G, S, and H were calculated using the van't Hoff's equation and Gibbs equation, and the results are shown in Table 4.

$$\Delta G^0 = -RT\, ln\, K_D \quad \text{(Equation 6)}$$

$$ln\, K_D = \frac{\Delta S^0}{R} - \frac{\Delta H^0}{RT} \quad \text{(Equation 7)}$$

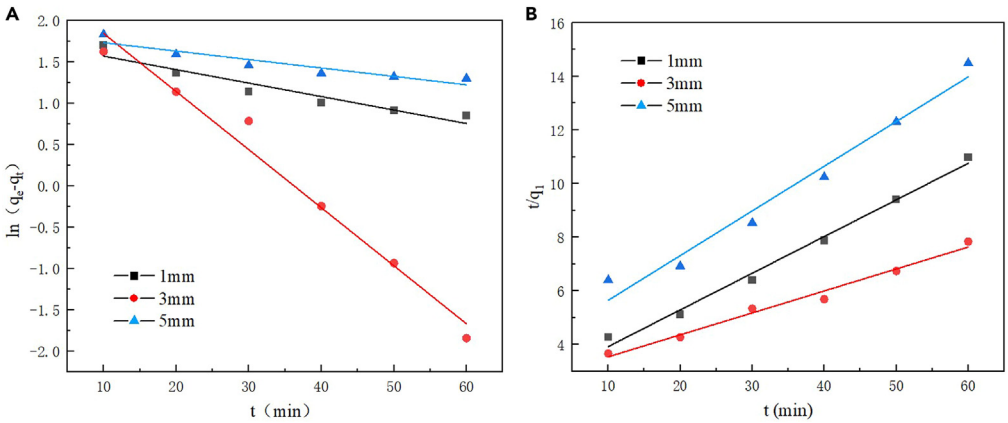

Figure 7. Fitting of adsorption kinetic model with different pole plate spacing

(A) Quasi-primary kinetic fitting results.

(B) Quasi-secondary kinetic fitting results.

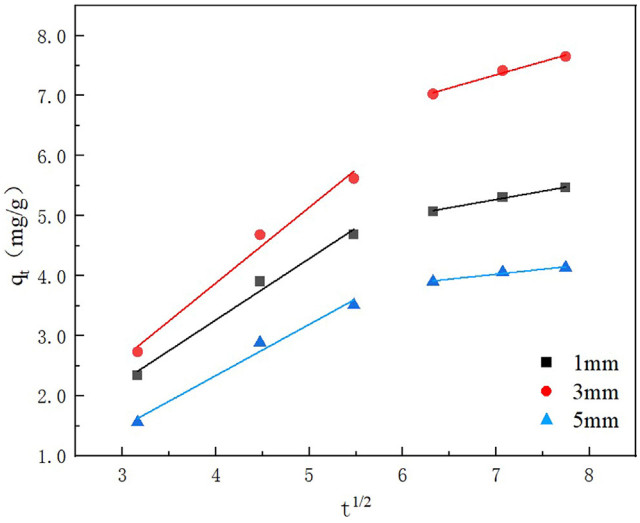

Figure 8. Fitting results of the intraparticle diffusion model

$$K_D = \frac{q_e}{C_e} \quad \text{(Equation 8)}$$

ΔG gradually decreases with increasing temperature and is positive, indicating that increasing temperature helps the adsorption reaction to occur. The ΔS and ΔH of this reaction are both positive, indicating that the adsorption reaction is a heat absorption process with an increase in entropy.

Adsorption cycle

The results of 10 adsorption-desorption cycles are shown in Figure 9, and the results were extrapolated 50 times using the extrapolation method and fitted to the equation.

The electrosorption efficiency gradually decreases over 10 adsorption cycles until it reaches the lowest points. As Figure 9A shows, the extrapolation calculations show that the adsorption efficiency will continue to decrease until the 50th time still retaining 75% of the treatment effect of the first adsorption. The fit of the equation for 50 cycles reached 0.9951, and the cyclic process of electroabsorption was considered to compound the first-order fitting equation. As Figure 9B shows, the first-order derivative of the equation achieves zero between 239 and 240, and the adsorption efficiency does not decrease indefinitely during the adsorption cycle and eventually stabilizes at about 75% of the initial adsorption efficiency.[45,46] The removal of Zn from wastewater by flow-through electroabsorption has certain practical significance, and its application effect in practical engineering can be investigated.

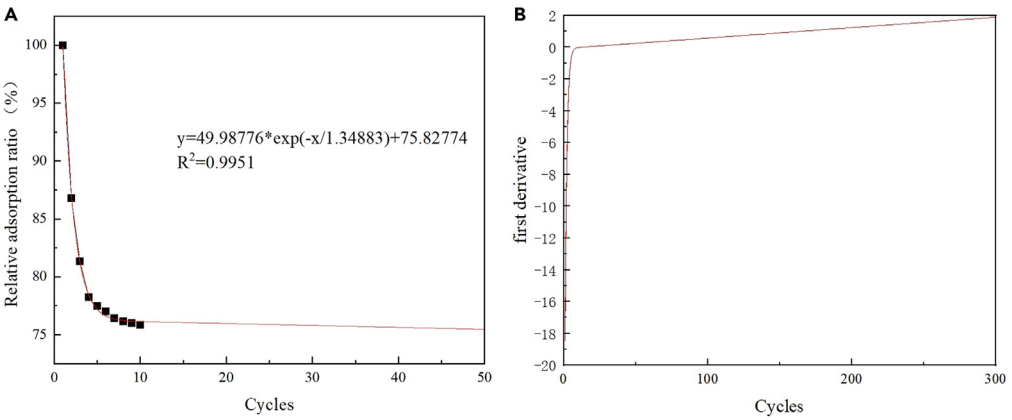

Figure 9. Adsorption cycle experimental results and first-order derivatives of the fitted equations

(A) Adsorption cycle and epitaxial fitting results.

(B) First-order derivatives of the fitted equations.

DISCUSSION

In this study, it is verified by experiments that the flow-through stacked electro-adsorption system has a good treatment capacity for Zn^{2+} wastewater under the condition that the adsorption capacity is renewable. The suitable working conditions for Zn removal from wastewater by flow-through electrosorption are 15°C, pH = 8, 3 mm pole plate spacing, and 2 V, and adsorption capacity of up to 24.79 mg/g. There is a limit loss of about 25% of the adsorption efficiency after several cycles, and the adsorption capacity does not decrease indefinitely. In dealing with wastewater Zn^{2+} pollution, or even heavy metal pollution, flow-through electroabsorption technology can be properly applied to treat produced water and protect the water environment.

With its high adsorption capacity and strong adsorbent regeneration ability, flow-through electro-adsorption technology can provide an economical and easy-to-use engineering method for industrial wastewater treatment, industrial desalination, deep purification of drinking water, brackish water desalination, seawater desalination, and other aspects in today's severe water pollution and water shortage. These experimental results may be helpful to better understand the working mechanism of the flow-through stacked electro-adsorption system in dealing with Zn^{2+} wastewater. Future research needs experimental study on the treatment efficiency of this system for different metal ions and their mixed solutions, and the development of separation and adsorption mechanisms, and fully compare the adsorption behavior under different flow patterns, to provide a theoretical basis for adsorption-separation and desorption-concentration of actual heavy metal industrial wastewater.

Limitations of the study

While our study demonstrates promising results, we also acknowledge some limitations that need to be addressed. Limited by the reactor shape, stacked flow-through reactors may be more prone to blockage, especially for wastewater to be treated, which requires a fine filter at the front end. Second, the currently employed reactor is relatively simple, and the stacking of multiple layers of electrodes inevitably produces phenomena such as local shorting. Third, the whole reaction system is still in a chaotic state in terms of the flow state, and the introduction of the means of computational fluid dynamics coupled with the computational electric field may help to solve this problem by exploring the state of the system including particle migration and adsorption.

STAR★METHODS

Detailed methods are provided in the online version of this paper and include the following:

- KEY RESOURCES TABLE
- RESOURCE AVAILABILITY
  - Lead contact
  - Materials availability
  - Data and code availability
- EXPERIMENTAL MODEL AND SUBJECT DETAILS
- METHOD DETAILS
  - Materials
  - Adsorption experiments
- QUANTIFICATION AND STATISTICAL ANALYSIS

ACKNOWLEDGMENTS

All authors declare no financial or non-financial competing interests.

AUTHOR CONTRIBUTIONS

Y.D. and M.J. conceptualized and designed the study. J.Z. and F.Z. analyzed the data. S.M. performed the investigation. Y.Z. drafted the manuscript. All authors read and approved the final manuscript and had final responsibility for the decision to submit for publication.

DECLARATION OF INTERESTS

The authors declare no competing interests.

Received: September 26, 2023
Revised: February 26, 2024
Accepted: March 14, 2024
Published: March 16, 2024

REFERENCES

1. McGinnis, R.L., and Elimelech, M. (2008). Global challenges in energy and water supply: the promise of engineered osmosis. Environ. Sci. Technol. *42*, 8625–8629. https://doi.org/10.1021/es800812m.
2. Tang, Z.L., Li, S.M., and Meng, Z.Z. (2015). Analysis on the Relation of Water Environment and Economic Development. Appl. Mech. Mater. *719–720*, 941–948. https://doi.org/10.4028/www.scientific.net/AMM.737.941.
3. Frank, A., Figueroa, F., Guerrero Victor, H., Daniela, N.-B., Ming, N., Camilo, Z.-L., and Ezequiel, Z.-L. (2021). Heavy metal water pollution: A fresh look at hazards, novel, and conventional remediation methods. Environ. Technol. Innovat. *22*, 1143–1154. https://doi.org/10.1016/J.ETI.2021.101504.
4. Vânia, C., Esteves Valdemar, I., Guilaine, J., and Otero, M. (2022). Overview of relevant economic and environmental aspects of waste-based activated carbons aimed at adsorptive water treatments. J. Clean. Prod. *344*, 1384–1410. https://doi.org/10.1016/J.JCLEPRO.2022.130984.
5. Zhao, F., Shan, R., Gu, J., Zhang, Y., Yuan, H., and Chen, Y. (2022). Magnetically Recyclable Loofah Biochar by $KMnO_4$ Modification for Adsorption of Cu (II) from Aqueous Solutions. ACS Omega *7*, 8844–8853. https://doi.org/10.1021/ACSOMEGA.1C07163.
6. Barad, J.M., Kohli, H.P., and Chakraborty, M. (2022). Adsorption of hexavalent chromium from the aqueous stream by maghemite nanoparticles synthesized by the microemulsion method. Energy Nexus *5*, 1035–1044. https://doi.org/10.1016/J.NEXUS.2021.100035.
7. Macías, G.A., Gómez, C.M., Alfaro, D.M., Alexandre, F.M., and Martínez, N.J. (2017). Study of the adsorption and electroabsorption process of Cu (II) ions within thermally and chemically modified activated carbon. J. Hazard Mater. *328*, 46–55. https://doi.org/10.1016/j.jhazmat.2016.11.036.
8. Cheng, Y., Shi, J., Zhang, Q., Fang, C., Chen, J., and Li, F. (2022). Recent Progresses in Adsorption Mechanism, Architectures, Electrode Materials and Applications for Advanced Electrosorption System: A Review. Polymers *14*, 2985. https://doi.org/10.3390/POLYM14152985.
9. Rychagov, A., Tripachev, O., Mikhalin, A., and Izmaylova, M. (2022). Capacitive characteristics and electrosorption of hydrogen in microporous activated carbon fibers. Int. J. Hydrogen Energy *47*, 10194–10203. https://doi.org/10.1016/J.IJHYDENE.2022.01.106.
10. Gupta, V., and Nayak, A. (2012). Cadmium removal and recovery from aqueous solutions by novel adsorbents prepared from orange peel and Fe_2O_3 nanoparticles. Chem. Eng. J. *180*, 81–90. https://doi.org/10.1016/j.cej.2011.11.006.
11. Morikubo, S., Kosaka, Y., Enomoto, D., Nishida, A., and Takuma, Y. (2021). Effect of ammonia stripping and influence of contaminants in zinc plating wastewater. J. Environ. Manag. *298*, 113459. https://doi.org/10.1016/J.JENVMAN.2021.113459.
12. Han, S., Shigeki, M., and Wataru, N. (2016). Impact of Bioavailability Incorporation on Ecological Risk Assessment of Nickel, Copper, and Zinc in Surface Waters. Water Air Soil Pollut. *227*, 480.1. https://doi.org/10.1007/s11270-016-3090-x.
13. Alkhadra, M.A., Su, X., Suss, M.E., Tian, H., Guyes, E.N., Shocron, A.N., Conforti, K.M., de Souza, J.P., Kim, N., Tedesco, M., et al. (2022). Electrochemical Methods for Water Purification, Ion Separations, and Energy Conversion. Chem. Rev. *122*, 13547–13635. https://doi.org/10.1021/ACS.CHEMREV.1C00396.
14. Chen, J., Hu, J., Jia, C.Q., Hailong, L., Song, C., and Junxian, X. (2022). Economical preparation of high-performance activated carbon fiber papers as self-supporting supercapacitor electrodes. Chem. Eng. J. *450*, 137–146. https://doi.org/10.1016/J.CEJ.2022.137938.
15. Zhu, L., Yao, Y., Chen, D., and Lan, P. (2022). The effective removal of Pb^{2+} by activated carbon fibers modified by l-cysteine: an exploration of kinetics, thermodynamics, and mechanism. RSC Adv. *12*, 20062–20073. https://doi.org/10.1039/D2RA01521H.
16. Datar, S.D., Raheman, S., Mane, R.S., Chavda, D., and Jha, N. (2022). Improved electrosorption performance using acid-treated electrode scaffold in capacitive deionization. Mater. Chem. Phys. *281*, 125–134. https://doi.org/10.1016/J.MATCHEMPHYS.2022.125851.
17. Kohli, H.P., Gupta, S., and Chakraborty, M. (2019). Stability and performance study of emulsion nanofluid membrane: A combined approach of adsorption and extraction of Ethylparaben. Colloids Surf. A Physicochem. Eng. Asp. *579*, 123675. https://doi.org/10.1016/j.colsurfa.2019.123675.
18. Shirasangi, R., Kohli, H.P., and Chakraborty, M. (2023). Stability of emulsion liquid membrane using blended nonionic surfactant and multi-walled carbon nanotubes (MWCNTs) for methylparaben removal. J. Dispersion Sci. Technol. *1*, 81–90. https://doi.org/10.1080/01932691.2023.2194393.
19. Yi, Z., Chen, Z., Yin, K., Wang, L., and Wang, K. (2023). Sensing as the key to the safety and sustainability of new energy storage devices. Prot. Control Mod. Power Syst. *8*, 27–307. https://doi.org/10.1186/S41601-023-00300-2.
20. Yu, X., Shang, Y., Zheng, L., and Wang, K. (2023). Application of Nanogenerators in the Field of Acoustics. Bioconjugate Chem. *5*, 5240–5248. https://doi.org/10.1021/acsaelm.3c00996.
21. Zhang, P., Ma, Y., Liu, B., and Zhang, H. (2024). Enhanced performance triboelectric nanogenerator based on mullite/PVA composites for self-driven sensing and smart home control. Smart Mater. Struct. *33*, 035003. https://doi.org/10.1088/1361-665X/AD21B4.
22. Phouthavong, V., Park, J., Nishihama, T., Yoshida, S., Hagio, T., Kamimoto, Y., and Ichino, R. (2022). Amine-Modified Small Pore Mesoporous Silica as Potential Adsorbent for Zn Removal from Plating Wastewater. Coatings *12*, 1258. https://doi.org/10.3390/COATINGS12091258.
23. Sun, J., Zhang, C., Song, Z., and Waite, T.D. (2022). Boron Removal from Reverse Osmosis Permeate Using an Electrosorption Process: Feasibility, Kinetics, and Mechanism. Environ. Sci. Technol. *56*, 10391–10401. https://doi.org/10.1021/ACS.EST.2C02297.
24. Fang, J., Jiang, R., Wang, Z., Zhang, W., and Zhang, K. (2017). Preparation of Aluminum Supported Activated Carbon Fiber Electrode for Adsorption of Phosphorus. J. Ceram. Soc. *45*, 1000–1009. https://doi.org/10.14062/j.issn.0454-5648.2017.07.17.
25. Ma, L., Huang, L., Xu, Y., Liu, C., Wang, F., Xing, H., and Ma, S. (2020). Dynamics and Model Research on the Electrosorption by Activated Carbon Fiber Electrodes. Water *13*, 62. https://doi.org/10.3390/W13010062.
26. Chai, Y., Qin, P., Wu, Z., Bai, M., Li, W., Pan, J., Cao, R., Chen, A., Jin, D., and Peng, C. (2021). A coupled system of flow-through electro-Fenton and electrosorption processes for the efficient treatment of high-salinity organic wastewater. Separ. Purif. Technol. *267*, 118683. https://doi.org/10.1016/J.SEPPUR.2021.118683.
27. Suen, N.T., Hung, S.F., Quan, Q., Zhang, N., Xu, Y., and Chen, H.M. (2017). Electrocatalysis for the oxygen evolution reaction: recent development and future perspectives. Chem. Soc. Rev. *46*, 337–365. https://doi.org/10.1039/c6cs00328a.
28. Duan, R., and Fedler, C.B. (2022). Competitive adsorption of Cu^{2+}, Pb^{2+}, Cd^{2+}, and Zn^{2+} onto water treatment residuals: implications for mobility in stormwater bioretention systems. Water Sci. Technol. *86*, 878–893. https://doi.org/10.2166/WST.2022.258.
29. Wang, Z., Ding, J., Razanajatovo, R.M., Huang, J., Zheng, L., Zou, H., Wang, Z., and Liu, J. (2022). Sorption of selected pharmaceutical compounds on polyethylene microplastics: Roles of pH, aging, and competitive sorption. Chemosphere *307*, 135561. https://doi.org/10.1016/J.CHEMOSPHERE.2022.135561.
30. He, S., Li, Y., Weng, L., Wang, J., He, J., Liu, Y., Zhang, K., Wu, Q., Zhang, Y., and Zhang, Z. (2018). Competitive adsorption of Cd^{2+}, Pb^{2+}, and Ni^{2+} onto Fe^{3+}-modified argillaceous limestone: Influence of pH, ionic strength and natural organic matters. Sci. Total Environ. *637–638*, 69–78. https://doi.org/10.1016/j.scitotenv.2018.04.300.
31. Wu, F., and Xie, S. (2023). The adsorption of U(VI) by persimmon tannin modified aminated polyacrylonitrile fiber. J. Phys, Conf. Ser. *2587*, 012031. https://doi.org/10.1088/1742-6596/2587/1/012031.
32. Stewart, G., Debrah, D., Paul, H., Lee, S.K., Schlegel, H., and Wen, B.L. (2023). Carrier-Envelope Phase Controlling of Ion Momentum Distributions in Strong Field Double Ionization of Methyl Iodide. J. Phys. Chem. A *127*, 54–67. https://doi.org/10.1021/ACS.JPCA.2C06754.
33. Li, H., Liu, L., and Liu, S. (2010). Effect of Electrostatic Field Originating from Charged Humic Surface on the Adsorption Kinetics of Zn^{2+}. J. Southwest Univ. *3*, 77–81. https://doi.org/10.13718/j.cnki.xdzk.2010.03.016.
34. Xing, Y., Chen, X., and Wang, D. (2007). Electrically regenerated ion exchange for removal and recovery of Cr (VI) from wastewater. Environ. Sci. Technol. *41*, 1439–1443. https://doi.org/10.1021/es061499l.
35. Kim, T., Dykstra, J.E., Porada, S., van der Wal, A., Yoon, J., and Biesheuvel, P.M. (2015). Enhanced charge efficiency and reduced energy use in capacitive deionization by increasing the discharge voltage. J. Colloid Interface Sci. *446*, 317–326. https://doi.org/10.1016/j.jcis.2014.08.041.
36. Chen, X., Wang, L., Ding, C., Xie, H., Zou, H., Deng, J., Liu, Z., Shi, J., and Ding, Y. (2024). Highly efficient removal of radioactive iodine

anions by nano silver modified activated carbon fiber. Appl. Surf. Sci. *643*, 158644. https://doi.org/10.1016/J.APSUSC.2023.158644.

37. Xue, Y., Cheng, W., Cao, M., Gao, J., Chen, J., Gui, Y., Zhu, W., and Ma, F. (2022). Development of nitric acid-modified activated carbon electrode for removal of Cosup^{2+}/sup/Mnsup^{2+}/sup/Nisup^{2+}/sup by electrosorption. Environ. Sci. Pollut. Res. Int. *29*, 77536–77552. https://doi.org/10.1007/S11356-022-21272-0.
38. Liang, X., Li, M., Wang, K., and Luo, G. (2022). Determination of Time-Evolving interfacial tension and ionic surfactant adsorption kinetics in the microfluidic droplet formation process. J. Colloid Interface Sci. *617*, 106–117. https://doi.org/10.1016/J.JCIS.2022.02.139.
39. Liu, X., Zhang, Y., Zhang, T., and Zhang, T. (2022). Magnetic red mud/chitosan-based bionanocomposites for adsorption of Cr (VI) from aqueous solutions: synthesis, characterization and adsorption kinetics. Polym. Bull. *80*, 2099–2118. https://doi.org/10.1007/S00289-022-04137-X.
40. Anjali, B., Shweta, C., Laxmi, G., and Maya, S. (2022). A hybrid bio-nanocomposite for Pb (II) ion removal from water: synthesis, characterization, and adsorption kinetics studies. Polym. Bull. *57*, 1–32. https://doi.org/10.1007/S00289-021-04073-2.
41. Silva, L.M., Muñoz-Peña, M.J., Domínguez-Vargas, J.R., González, T., and Silva Luís, M.S. (2021). Kinetic and equilibrium adsorption parameters estimation based on a heterogeneous intraparticle diffusion model. Surface. Interfac. *22*, 100791–100799. https://doi.org/10.1016/j.surfin.2020.100791.
42. Jeyaseelan, A., Iiango, A.K., Naushad, M., and Viswanathan, N. (2023). Enhanced and fast fluoride adsorption using cerium organic frameworks based hydrotalcite hybrid material. J. Rare Earths *12*, 2010–2017. https://doi.org/10.1016/J.JRE.2022.09.023.
43. Kumar, S., Dumpala, R.M.R., Chandane, A., and Bahadur, J. (2022). Elucidation of the sorbent role in sorption thermodynamics of uranium (VI) on goethite. Environ. Sci. Process. Impacts *24*, 567–575. https://doi.org/10.1039/D1EM00380A.
44. Priyanka, K., Kumar, S.A., and Kumar, V.V. (2022). Efficacy of rice straw derived biochar for removal of Pb^{2+} and Zn^{2+} from aqueous: Adsorption, thermodynamic and cost analysis. Bioresour. Technol. Rep. *17*, 920–935. https://doi.org/10.1016/J.BITEB.2021.100920.
45. Ning, K., Wang, J., Zeng, X., Liu, X., Yu, R., and Zhao, Z. (2022). Organic removal from coal-to-chemical brine by a multistage system of adsorption-regeneration and electrochemically driven UV/chlorine processes. J. Hazard Mater. *430*, 128379. https://doi.org/10.1016/J.JHAZMAT.2022.128379.
46. Wang, H., Henghui, Y., Wu, G., Lei, H., Jia, Y., Liu, X., and Zhang, H. (2023). Co/Fe co-doped ZIF-8 derived hierarchically porous composites as high-performance electrode materials for Cu^{2+} ions capacitive deionization. Chem. Eng. J. *15*, 388–397. https://doi.org/10.1016/j.cej.2023.141621.

STAR★METHODS

KEY RESOURCES TABLE

REAGENT or RESOURCE	SOURCE	IDENTIFIER
Chemicals, peptides, and recombinant proteins		
Activated carbon fiber mat	ST-2000, SENYOU Co., CHINA	customized
zinc sulphate	China National Medicine Group	7733-02-0
Software and algorithms		
IBM SPSS Statistics (version 26.0)	IBM SPSS Statistics software	https://www.ibm.com/cn-zh/products/spss-statistics

RESOURCE AVAILABILITY

Lead contact

Further information and requests for resources should be directed to and will be fulfilled by the Lead Contact, Yusen Dong (18810887900@163. com).

Materials availability

This study did not generate new unique reagents.

Data and code availability

Data reported in this paper will be shared by the lead contact upon request.

This paper does not report original code.

Any additional information required to reanalyze the data reported in this paper is available from the lead contact upon request.

EXPERIMENTAL MODEL AND SUBJECT DETAILS

No experimental models (animals, human subjects, plants, microbe strains, cell lines, primary cell cultures) were used in the study.

METHOD DETAILS

Materials

Activated carbon fiber mat (ST-2000, SENYOU Co., CHINA) has a specific surface area of 1800-2000m^2/g, static adsorption capacity for benzene of 70-80 (wt%), pores volume of 0.8-1.2ml/g, and average pore diameter of 1.7-2nm. Data analysis in the text was done using spss 26.0 (IBM Co., American).

Adsorption experiments

The reactor used in the experiment is shown in Figure 1. The reactor is a cylindrical flow-through structure (Place in water bath at desired temperature) with an internal stack of electrodes that fills the entire fluid cross-section, and all fluids run through the fluid from bottom to top. The electrode stack is a cathode-ACF-dielectric-anode-dielectric-ACF-cathode cycle stack (three cycles in total). The cathode and anode plates are made of titanium to ensure stability and the dielectric is a plastic mesh to ensure insulation effectiveness. The raw water tank is placed on a thermostatic heater to ensure the required inlet water temperature for the experiment.

The electrosorption performance of the flow-through activated carbon electrosorption reactor was evaluated by the adsorption and desorption behaviors of Zn^{2+} in the flow-through reactor. The effects of different pole plate spacing (1-5mm), voltage (1.2-2.5V), pH (1-9), temperature (15-35°C), and feed water (10mg/L-400mg/L)(Typical electroplating plant wastewater after homogenization before treatment, the concentration of Zn^{2+} is often 10-400 mg/L) concentration on the adsorption of Zn^{2+} by activated carbon fiber mats were investigated. The experimental reactor has 6 layers of cathodes with activated carbon fiber mats on both sides and 7 layers of anodes.

To study the adsorption kinetics, electroabsorption tests were performed with Zn^{2+} solutions of 400 mg/L and pH 8 at a voltage of 2.0 V, pole plate spacing of 1, 3, and 5 mm, and under hydrostatic conditions, and the produced water was taken at 10, 20, 30, 40, 50, and 60 min, respectively. The Zn^{2+} concentration was determined after filtration (0.45 μm).

To study the thermodynamics of electro-adsorption, the electro-adsorption reaction was carried out under the conditions of pH 8, 400 mg/L, reaction voltage 2 V, and hydrostatic pressure for 2 hours. The temperature gradients were 15°C, 25°C, and 35°C. The supernatant (0.45 μ m) was filtered and the concentration of Zn^{2+} was determined.

To study the adsorption cycle, electroabsorption experiments were carried out under the conditions of a voltage of 2V, pH of 8, a water temperature of 20°C, pole plate spacing of 3mm, and Zn^{2+} concentration of 400mg/L. The current direction was changed every hour and a total of 10 cycles were carried out.

QUANTIFICATION AND STATISTICAL ANALYSIS

Spss software was used in statistical analysis.

Correlation analysis method is used, as shown in Tables 1, 2, 3, 4, and 5. The results of regression analysis can be seen in Figures 7, 8, and 9 and below figures and tables.

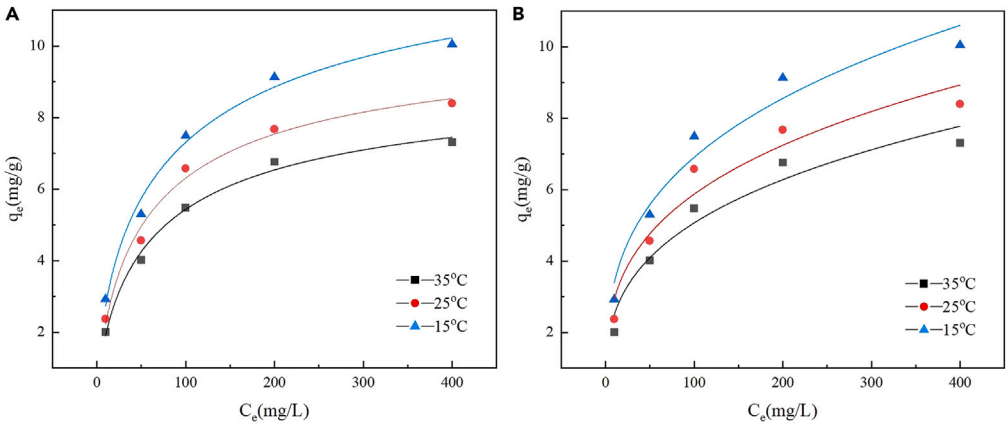

Fitting curves of Langmuir (A) and Freundlich (B) adsorption isotherm models

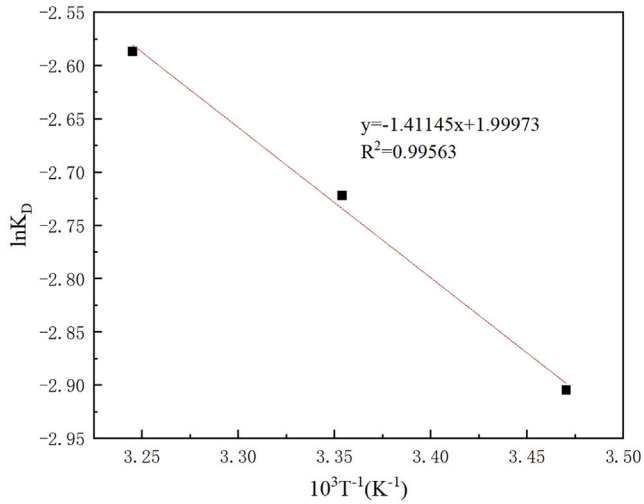

Graph of 102lnKD versus 103T-1

Dynamical fitting parameters			
Pole plate pitch	q_e	k	R^2
First order dynamics			
1 mm	5.6589	0.01631	0.891
3 mm	12.7705	0.07028	0.972
5 mm	6.2647	0.0102	0.841
Second order dynamics			
1 mm	7.3083	0.007329	0.989
3 mm	12.2070	0.002466	0.980
5 mm	5.9988	0.006975	0.966

Parameters for fitting the intraparticle diffusion model						
Pole plate pitch	c_1	k_1	R_1^2	c_2	k_2	R_2^2
1 mm	−0.818	1.021	0.974	3.343	0.275	0.985
3 mm	−1.16	1.26	0.969	4.259	0.441	0.974
5 mm	−1.068	0.852	0.967	2.868	0.166	0.949

Adsorption thermodynamic fitting parameters			
T/(°C)	q_m	K_f	R^2
Langmuir			
15	14.04009	0.05375	0.97782
25	10.60852	0.04794	0.97671
35	9.42945	0.04685	0.98546
T/(°C)	1/n	K_f	R^2
Freundlich			
15	0.30921	1.66177	0.94941
25	0.30245	1.45781	0.92786
35	0.30893	1.2209	0.9382

Values of thermodynamic fitting parameters at different temperatures				
T/(^{O}C)	$\ln K_D$	ΔG^0/(KJ·mol^{-1})	ΔH^0/(KJ·mol^{-1})	ΔS^0/(J·mol^{-1}·K^{-1})
15	−2.904	6.958	11.720	16.525
25	−2.722	6.748	11.720	16.525
35	−2.587	6.628	11.720	16.525